European Spine Journal
https://doi.org/10.1007/s00586-023-08024-5

REVIEW ARTICLE

Deep learning algorithm for automatically measuring Cobb angle in patients with idiopathic scoliosis

Ming Xing Wang[1] · Jeoung Kun Kim[1] · Jin-Woo Choi[2] · Donghwi Park[3] · Min Cheol Chang[4]

Received: 19 June 2023 / Revised: 30 August 2023 / Accepted: 25 October 2023

Abstract

Purpose The Cobb angle is a standard measurement to qualify and track the progression of scoliosis. However, the Cobb angle has high inter- and intra-observer variability. Consequently, its measurement varies with vertebrae and may even differ when the same vertebra is measured. Therefore, it is not constant and differs with measurements. This study aimed to develop a deep learning model that automatically measures the Cobb angle. The deep learning model for identifying vertebrae on spine radiographs was developed.

Methods The dataset consisted of 297 images that were divided into two subsets for training and validation. Two hundred and twenty-seven images (76.4%) were used to train the model, while 70 images (23.6%) were used as the validation dataset. Absolut error between the measurements by the observer and developed deep learning model and intraclass correlation coefficient (ICC).

Results The average absolute error between the measurements was 1.97° with a standard deviation of 1.57°. In addition, 95.9% of the angles had an absolute error of less than 5°. The ICC was calculated to assess the model's reliability further. The ICC was 0.981, indicating excellent reliability.

Conclusions The authors believe the model will be useful in clinical practice by relieving clinicians of the burden of having to manually compute the Cobb angle. Further studies are needed to enhance the accuracy and versatility of this deep learning model.

Keywords Deep learning · Scoliosis · Cobb angle · Spine

Introduction

Scoliosis is an abnormal lateral curvature of the spine that may rotate or twist vertically [1]. The incidence of scoliosis is 2–4% in children aged 10 and 16 years [1]. Scoliosis is classified into four types: (1) idiopathic (the most common); (2) congenital; (3) neuromuscular; and (4) degenerative [2]. "Idiopathic" denotes an unknown etiology. Idiopathic scoliosis may be divided based on onset into early onset (age 5–7) and late onset (age 7 until maturity) [3]. It may also be divided based on phase into infantile, juvenile, and adolescent [4]. Scoliosis is diagnosed by determining standing coronal curvature on a posterior-anterior spine radiograph [2]. Cobb angles qualify and track scoliosis progression. It is the angle between the upper border of the most tilted upper vertebra and the lower border of the most tilted lowest vertebra [5].

Until skeletal maturation, a rigid brace conservatively controls scoliosis progression when the Cobb angle

Ming Xing Wang and Jeoung Kun Kim have contributed equally to this study as co-first authors.

✉ Donghwi Park
bdome@hanmail.net

✉ Min Cheol Chang
wheel633@ynu.ac.kr

[1] Department of Business Administration, School of Business, Yeungnam University, Gyeongsan-Si, Republic of Korea

[2] Department of Physical Medicine and Rehabilitation, Ulsan University Hospital, University of Ulsan College of Medicine, Ulsan, Republic of Korea

[3] Department of Rehabilitation Medicine, Daegu Fatima Hospital, Ayangro 99, Dong Gu, Daegu 41199, Republic of Korea

[4] Department of Physical Medicine and Rehabilitation, College of Medicine, Yeungnam University, 317-1, Daemyungdong, Namku, Daegu 705-717, Republic of Korea

Published online: 17 February 2024

is > 20° or 25° [6]. When the Cobb angle is > 40º or 50º, spinal fusion may prevent severe scoliosis complications, including cardiopulmonary dysfunction, back pain, and limited physical activity [7]. Early diagnosis and appropriate management prevent curve progression. Clinically, children with scoliosis are regularly monitored with serial radiographs.

The measurements of the Cobb angle are not constant. The Cobb angle measurement varies between vertebrae and even within the same vertebra [5]. Deep learning techniques automatically learn feature representations from provided data through trial and error, extracting meaningful information [8–10], thus significantly improving object detection [11]. Object detection, therefore, determines instances of objects from specified categories in an image. Once objects are detected, each object instance's spatial location and extent are returned via a bounding box [11]. Object detection, as the foundation of image comprehension and computer vision, is the foundation for solving complex or high-level vision tasks such as segmentation, object tracking, image captioning, activity recognition, and event detection [11]. Object detection is used in medical imaging to identify pathologies like pneumonia, malignancy, and bone fractures [12, 13]. Therefore, object detection may be useful for lumbar vertebrae detection and Cobb angle measurement.

In this study, a deep learning model that automatically measures the Cobb angle was developed.

Methods

Participants

This study was approved by the ethics committee of Ulsan University Hospital (2022-04-037). Patients' data referred to or visiting the Ulsan University Hospital for scoliosis screening between 2010 and 2022 were retrospectively reviewed. Standing anteroposterior whole spine radiographs of the included patients were used to develop the algorithm.

The inclusion criteria for this study were: (I) patients with a standing anteroposterior whole spine radiograph; and (II) patients aged 4–18. The exclusion criteria were: (I) spine radiograms with interferences from extracorporeal objects; and (II) spine radiograms with spinal implants. Spine radiographs were retrieved from the institution's picture archiving and communication system (PACS), anonymized, and exported as JPEG images. For 70 of 297 whole spine radiographs, the Cobb angles were measured to validate the deep learning model's analysis. Each spine radiograph's Cobb angle was measured by (1) two blinded physiatrists (Observer 1, a scoliosis specialist, and Observer 2, a resident) and (2) deep learning models using the PACS's built-in function. Physiatrists individually measured Cobb angle analysis time of whole spine radiographs. Multiple Cobb angles may be obtained from a single spine radiograph. In this study, however, only the two largest Cobb angles were measured. Therefore, 70 images with 140 Cobb angles were measured by physiatrists. Additionally, physiatrists also determined the apex for spinal curvatures represented by each Cobb angle. The two largest Cobb angles and the apex were measured from spine radiographs.

In this study, a deep learning model predicated on MMRotate was employed. The model is an open-source toolbox designed for detecting rotated objects using the PyTorch framework. As a component of the OpenMMLab initiative, MMRotate amalgamates notable algorithms for rotated object detection, including ReDet, faster_rcnn, and oriented_reppoints. Since the performance of ReDet on the DOTA1.0 dataset was remarkable, with a mean average precision (mAP) of 79.87%, it was selected as the model for vertebrae detection in this study. Figure 1 illustrates the automated vertebrae identification method for Cobb angle computation.

Experiment

Vertebral detection experimental details

A deep learning model for identifying vertebra on spine radiographs was developed using Python 3.8, PyTorch 1.12.0, and CUDA 11.6. The model was trained using full training (unfreezing all layers) and transfer learning techniques. The stochastic gradient descent (SGD) optimizer was used to optimize the network. The dataset consisted of 297 images, split into two subsets for training and validation. Specifically, 227 images (76.4%) were used for training the model, while 70 images (23.6%) were used as the validation dataset.

We used the RandomFlip augmentation method to optimize the training process for all three axes (horizontal, vertical, and diagonal). Additionally, we configured the learning rate to 0.001 and implemented a warm-up approach with parameters type = "linear," warmup_iters = 500, warmup_ratio = 0.3333333333333333, and step = [75, 150]. This approach allowed the model's learning rate to increase gradually from a lower value to 0.001 during the initial 500 iterations. This was followed by a reduction to 0.0001 at 75 epochs and was maintained until training was completed. The adjustments in the learning rate during the first 1,000 iterations are illustrated in Figure A (Appendix 1), while Figure B (Appendix 1) delineates the temporal variations in the learning rate throughout model training. The model was configured with an input size of (1,024,1024) and underwent 150 training epochs. The mean average precision (mAP) served as the evaluation metric for the validation dataset, gaging the model's performance. A comprehensive overview

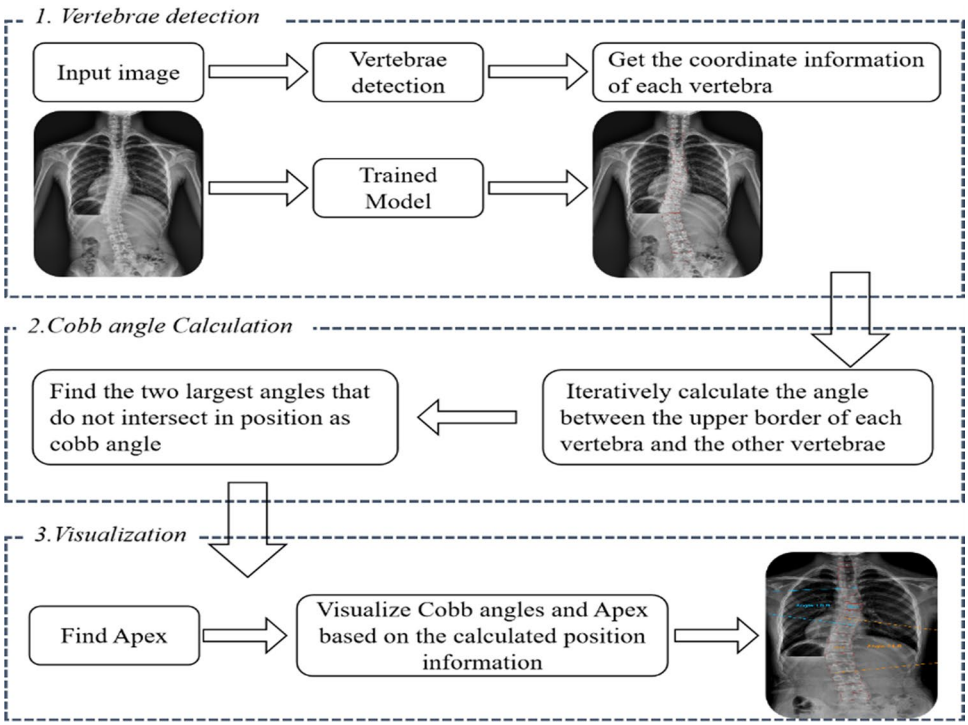

Fig. 1 Automated vertebrae detection and Cobb angle measurement procedure

of the experimental hyperparameters is shown in Table A in Appendix 1.

Of note, hyperparameters were selected using a comprehensive analysis of the model's performance in the validation set. The hyperparameters were fine-tuned to achieve a balance between accuracy and computational efficiency. The resulting model demonstrated outstanding performance in accurately identifying vertebrae on spinal radiographs.

Vertebra detection results

The model's performance was evaluated using mAP with intersection over union set to 0.5 (mAP_0.5). The results indicate that the model's highest performance was achieved at a best/mAP_0.5 score of 0.9054 in the validation dataset. Appendix 1 contains Figures C and D, which illustrate the alterations in mAP throughout the training process for the training and validation datasets, correspondingly.

The mAP_0.5 metric is a widely accepted performance measure for object detection tasks, and it reflects the model's ability to detect objects in images accurately. The high mAP_0.5 score achieved by our model in the validation dataset indicates its superior ability to identify vertebrae on spine radiographs.

mAP values were continuously monitored during training to ensure that the model was not overfitting the training dataset. The model achieved a satisfactory balance between its high accuracy and generalization ability. This was evidenced by its high mAP_0.5 score on the validation dataset.

To enhance the elucidation of our experimental findings, four annotated validation images and their respective detection outcomes have been supplied. Figure 2a displays radiographs of all subjects included in the validation dataset, featuring 17 vertebrae delineated by green rectangular bounding boxes. For the purpose of vertebra identification, identical images were utilized, as illustrated in Fig. 2b, where the detection outcomes are represented by red rectangular boxes. It is important to highlight that all detections were carried out with a notably high confidence level of 0.99.

Based on these results, it was concluded that the ReDet model could accurately identify vertebrae on spine radiographs. Likewise, the high-confidence detection results indicate that the model detected vertebrae in the images with a high level of accuracy. Visualization of the detection results provided a concrete representation of the model's performance that was more intuitive. These results further supported our evaluation and analysis of the model's effectiveness in identifying vertebrae on spine radiographs.

Cobb angle computation

A. Eliminating outliers

After the detection process, the model provided the location of each rotated bounding box for the 17 vertebrae in the form of [×1, y1, ×2, y2, ×3, y3, ×4, y4, confidence]. The points (×1, y1), (×2, y2), (×3, y3), and (×4,

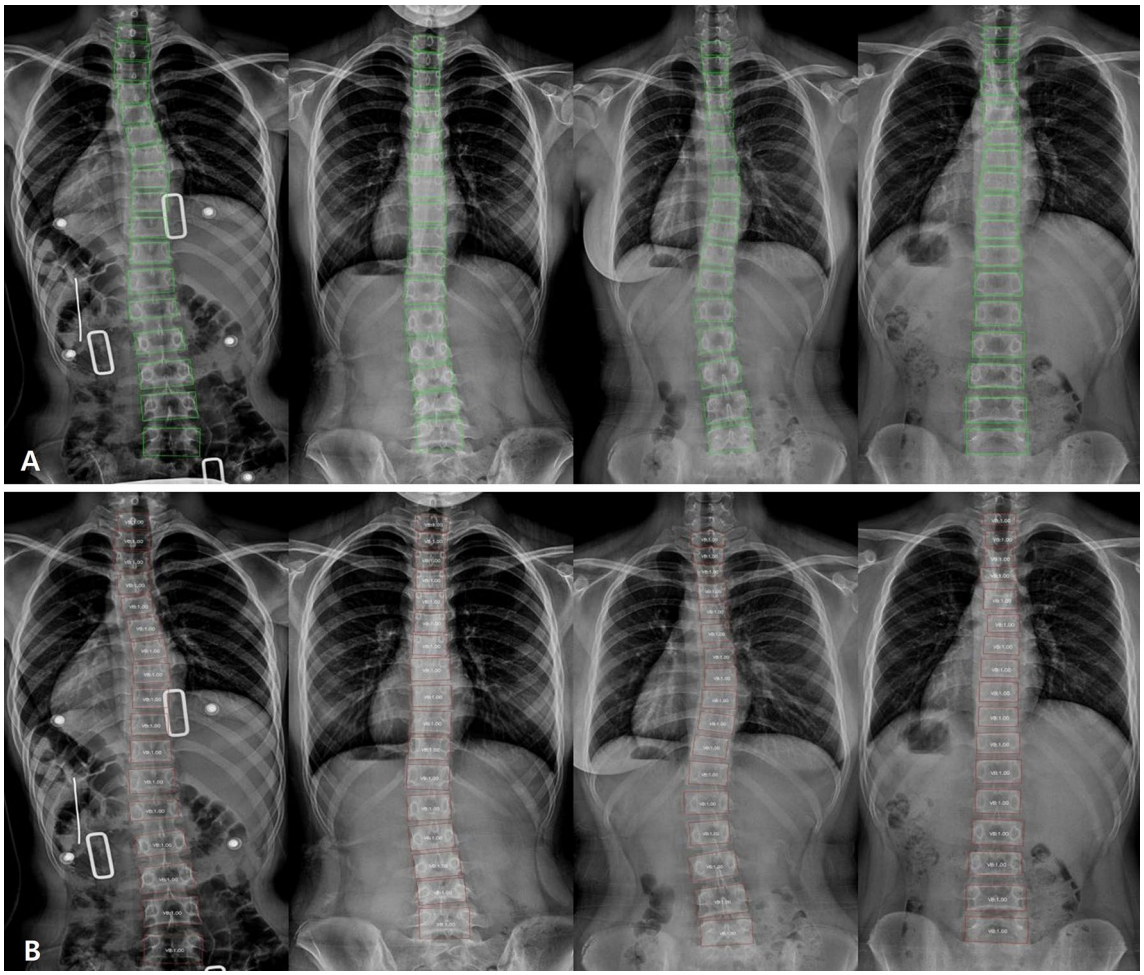

Fig. 2 Four annotated validation images and vertebra detection results

y4) represent the left bottom, left top, right top, and right bottom points of the bounding box, respectively.

Two main methods were used to remove potential outliers. The first method involved setting a confidence threshold so that bounding boxes with confidence scores below a certain threshold were considered outliers and excluded from the results. For this experiment, a confidence threshold of 0.5 was used.

The second method involved setting a distance threshold between a single bounding box and a set of bounding boxes. When the distance between a bounding box and its neighboring bounding boxes was greater than the threshold, the bounding box was considered an outlier and excluded from the results. For this experiment, the distance threshold was 2 times the standard deviation.

By applying the two methods, the majority of outliers were successfully eliminated. Therefore, robust and accurate bounding boxes for vertebrae were included. These steps ensured that the final results were reliable and accurate. The elimination process also provided a sound basis for further analysis and clinical use of the ReDet model.

B. Identifying Cobb angle

After eliminating outliers, the remaining bounding boxes were sorted based on their y1 coordinates. Thus, the vertebrae were ranked from T1 to L5. A value of K was assumed to determine the slope of the upper border line of each bounding box (formed by the left and right top points). Using this value, the slope of the upper borderline for each bounding box was calculated to refine the vertebrae detection results further. The formula used is shown as follows:

$$k = \left| \frac{y3 - y2}{x3 - x2} \right|$$

Accordingly, a list of slope values, Ks = [K1, K2, K3,…, K15, K16, K17], were easily computed. The angle (θ) between two lines with slopes Ki and Kj was computed using the following formula:

$$\theta = \arctan\left(\left|\frac{ki - kj}{1 + ki * kj}\right|\right)$$

The Cobb angle was calculated through iterative computation of the angles between K1 and K2, K1 and K3, K1 and K4, K1, and Ki, and so on, as illustrated in Fig. 2 B. Following this, the maximum non-overlapping angle was discerned. In their research, Sun et al. [14] utilized an identical method to determine the Cobb angle. Figure 3 depicts the algorithmic methodology and computational process for determining the Cobb angle by utilizing identified coordinates for vertebral bodies.

Based on our analyses, it was determined that three distinct angles could be detected (Table 1). The first angle, angle1, has a value of 15.7° and extends from the upper border of T10 to the lower border of L2. The second angle, angle2, has a value of 7.7° and spans from the upper border of T1 to the lower border of T10. Conventionally, the two largest angles are recognized as the Cobb angles.

C. Identifying the apex

To determine the apex of the spine curvature, the deepest point of the curve was identified [15]. This was done by first obtaining the center point (c_x, x_y) of each bounding box to serve as the representative of the box. Next, the cross point (cross_x, cross_y) of the two border lines of the Cobb angle was determined to obtain the point (×0, y0) on the line where the Cobb angle could be evenly divided. Subsequently, the center point closest to the point (×0, y0) was identified, and the vertebra on which this center point sat was regarded as the apex. The relevant formulae used in this computation are presented as follows:

$$x0 = (x1 - \text{cross\_}x)\cos\left(\frac{\theta}{2}\right) - (y1 - \text{cross\_}y)\sin\left(\frac{\theta}{2}\right) + \text{cross\_}x$$

$$y0 = (y1 - \text{cross\_}y)\cos\left(\frac{\theta}{2}\right) - (x1 - \text{cross\_}x)\sin\left(\frac{\theta}{2}\right) + \text{cross\_}y$$

$$\text{Min}\left(\sqrt{(c\_x - x0)^2 + (c\_x - y0)^2}\right)$$

Table 1 Initial results of cobb angle measurement

No	Angles	Upper vertebra	Lower vertebra
1	15.7	9 (T10)	13 (L2)
2	7.7	0 (T1)	9 (T10)
3	6.9	13 (L2)	16 (L5)

Statistical analysis

Statistical analyses were performed using SPSS software version 27. The mean absolute error and the proportion of Cobb angle measurements within a 5° deviation were

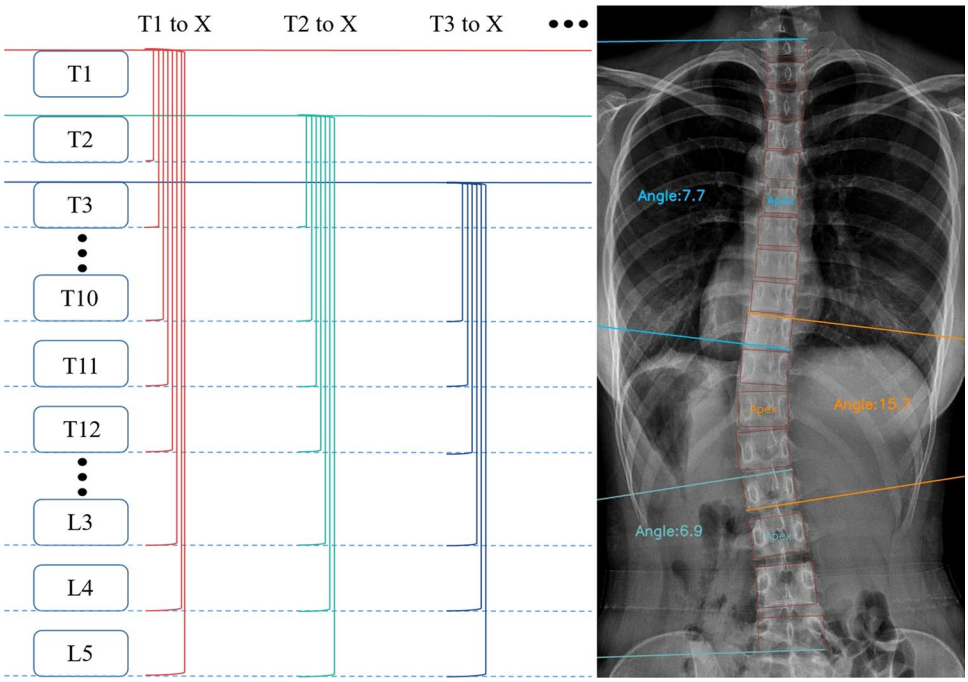

Fig. 3 The process for computing the Cobb angle traversal and a visualization of the resulting measurement of the Cobb angle

compared with two observers' measurements to assess the accuracy of the proposed model. The model's reliability was evaluated by calculating the intraclass correlation coefficient (ICC) and Pearson correlation coefficient (PCC). ICC reliability classifications were defined as poor (< 0.50), fair (0.50–0.75), good (> 0.75–0.90), and excellent (> 0.90). A significance threshold of $p < 0.05$ was established for this study.

To ensure greater validation reliability, we classified the Cobb angles into two distinct groups: cases where the angle exceeded 20° (referred to as the high-degree curve group), and cases where the angle measured 20° or less (labeled as the low-degree curve group). Subsequent analyses were conducted based on this categorization.

Results

This study evaluated the proposed model's performance in measuring the Cobb angle. The outcomes were compared with those obtained by the two observers. The results are presented in Appendix 2. The positions of the Cobb angles were initially compared based on the apex location to assess the similarities between the model and observer measurements. If the discrepancy between the expert's apex and the model's apex was less than 3, the angles were deemed identical. The model failed to identify one angle out of 70 images with 140 angles (false negative). Eight angles (false positives) had significant deviations in position. Considerable deviations in location were noted in the resident's measurements for 25 angles. The accuracy of the measurements made by the model and the resident was 93.57% and 82.14%, respectively. The measurement time, mean absolute error, and proportion of Cobb angle estimations within a 5° range were computed and compared with Observer 1's measurements.

To assess the reliability of our model, we calculated the ICC. The ICC was 0.981, indicating excellent reliability. The PCC showed a significant correlation (0.962, $p < 0.001$) between our model and the expert measurements. Our model outperformed Observer 2, who had ICC and PCC values of 0.924 and 0.860 ($p < 0.01$), respectively (Table 2). In the absolute error and percentage of error within 5°, our model showed a higher concordance rate with observer 1, a scoliosis specialist, than with observer 2, a resident (Table 2).

To enhance the clarity of the experimental results, we have provided 12 samples from the validation dataset with Cobb angles marked in Appendix 3.

Out of the 140 Cobb angles measured from 70 patients, there were instances where the diagnosed apex differed among observer 1, observer 2, and the proposed model. Thus, to validate the performance of our model classified into high- and low-degree curve groups, we exclusively used cases where the apex was consistent.

Tables 3 and 4 present the results of the comparison among observer 1, observer 2, and the proposed model, demonstrating the level of agreement in the measurements. For Cobb angle measurements of the high-degree curve

Table 2 A comparative analysis of cobb angle measurements: observer 1 vs (proposed model and observer 2)

Variables	Observer 1	Observer 2	Proposed model
Cobb angle (Mean/SD)	12.00 (8.44)	13.29 (9.06)	12.94 (8.52)
Measurement time (Sec, Mean/range)	57.80 (42–88)	54.37 (36–97)	2.21 (0.95–4.7)
Absolute error (Mean/SD)	–	2.88 (2.32)	1.97 (1.57)
Percentage of error within 5°	–	80.87%	95.9%
Intraclass correlation coefficient (ICC)	–	0.924	0.981
Pearson correlation coefficient (PCC)	–	0.860 ($P < 0.01$)	0.962 ($p < 0.001$)

SD standard deviation, *ICC* intraclass correlation coefficient, *PCC* Pearson correlation coefficient

Table 3 A comparative study of cobb angle measurements classified into high- and low-degree curves: observer 1 versus observer 2

Variables	High-degree curve (> 20°, 24 cases)		Low-degree curve (≤ 20°, 91 cases)	
	Observer 1	Observer 2	Observer 1	Observer 2
Cobb Angle (Mean/SD)	26.45 (5.90)	26.85 (8.08)	9.11 (4.41)	10.67 (4.76)
AE(Mean/SD)	_	2.69 (2.33)	_	2.92 (2.32)
Percent of Error within 5°	_	87.5%	_	79.6%
ICC	_	0.871	_	0.723
PCC	_	0.915 ($p < 0.01$)	_	0.725 ($P < 0.01$)

SD standard deviation, *AE* absolute error, *ICC* intraclass correlation coefficient, *PCC* Pearson correlation coefficient

Table 4 A comparative study of cobb angle measurements classified into high- and low-degree curves: observer 1 versus proposed model

Variables	High degree curve (> 20°, 25 cases)		Low degree curve (≤ 20°, 96 cases)	
	Observer 1	Proposed model	Observer 1	Proposed model
Cobb angle (mean/SD)	26.19 (5.91)	26.94 (7.45)	8.65 (4.58)	9.63 (4.41)
AE (mean/SD)	_	2.60 (1.64)	_	1.81 (1.52)
Percent of error within 5°	_	96%	_	95.3%
ICC	_	0.899	_	0.885
PCC	_	0.923 ($p < 0.01$)	_	0.885 ($p < 0.01$)

SD standard deviation, *AE* absolute error, *ICC* intraclass correlation coefficient, *PCC* Pearson correlation coefficient

group, both observer 2 and the proposed model exhibited a robust correlation and agreement with the measurements of observer 1. However, the proposed model surpassed observer 2 in terms of reduced absolute error and a greater proportion of measurements within a 5° range of the reference measurements. This implies that the proposed model could serve as a precise and reliable substitute for manual measurement, potentially enhancing clinical precision and decision-making for Cobb angles exceeding 20°.

Regarding Cobb angle measurements of 20° or less, both observer 2 and the proposed model consistently exhibited notable agreement and correlation with observer 1's measurements. However, the proposed model consistently outperformed observer 2 in performance. The model demonstrated a reduced absolute error and a greater proportion of measurements within a 5° range of the reference measurements. These findings suggest that the proposed model offers a more consistent and precise approach for measuring Cobb angles of 20° or less.

In both scenarios, the proposed model consistently outperformed observer 2 in terms of precision, accuracy, and the proportion of measurements within a 5° range of the reference measurements. The model exhibited a robust correlation and agreement with the scoliosis specialist's measurements. While observer 2's measurements showed moderate agreement and correlation, the proposed model excelled in terms of accuracy and consistency. This suggests that the proposed model is a reliable instrument for measuring Cobb angles.

Discussion

In this study, we developed an algorithm to measure the Cobb angle in children with scoliosis automatically. Our algorithm achieved an average absolute error of 1.97°, with 95.9% of the angles demonstrating an absolute error of less than 5°. Considering that Cobb angle measurements of less than 5° are generally regarded as within the normal measurement variability, we can consider the performance of our algorithm to be excellent [16]. The ICC was 0.981, indicating the model's excellent reliability. Additionally, a high correlation was observed, with a PCC of 0.962.

Currently, Cobb angle measurements are the gold standard for assessing the severity of scoliosis. Manual measurement often results in random errors in vertebral endplate localization and identification in clinical settings [5]. Additionally, the manual approach is time-consuming. To address these challenges, Pan et al. [17] developed computer-aided methods aimed at minimizing human intervention in measuring Cobb angles. In these systems, clinicians manually designate and label the curve's upper and lower-end vertebra on radiographs. Despite high accuracy comparable to experienced clinicians, clinicians' manual determination and labeling of the end vertebra remains an inevitable limitation.

Deep learning algorithms that measure the Cobb angle automatically have been proposed to overcome semi-automated system limitations. In a study conducted by Pan et al. in 2019 [17], two mask region-based convolutional neural network (CNN) models were employed to semi-automatically diagnose scoliosis and measure the Cobb angle on chest radiographs. Algorithms were developed from 248 lung cancer screening chest radiographs. The computer-aided and manual Cobb angle measurements had an ICC of 0.854 and a mean absolute error of 3.32°. Additionally, the sensitivity and specificity for diagnosing scoliosis on chest radiographs were 89.59% and 70.37%, respectively.

Also, in 2019, Horng et al. developed a CNN model to measure the Cobb angle from radiographs [18]. 10% of 1,000 augmented vertebrae images from 35 anterior–posterior spinal radiographs were randomly selected for validation. The model's performance was evaluated by comparing its results with those obtained manually by an expert and a novice. The ICC and PCC between the expert and novice were found to be 0.936 and 0.944, respectively. The ICC and PCC values between the model and the expert were 0.971, indicating a substantial agreement between the model's output and manual assessment.

Sun et al. developed an automated Cobb angle measurement algorithm in 2022 using 181 anterior–posterior spinal

radiographs, 145 of which were used for training and 36 for testing [14]. Two CNN-based deep-learning object detection models identified vertebral endplates and segmented each vertebra. The Cobb angle was then computed from the object detection model output, with the algorithm's reliability and correlation evaluated through the ICC and PCC, respectively. The ICC and PCC were 0.994 and 0.984, respectively. Our model's ICC and PCC values were slightly lower than Sun et al.'s, but it is promising for automated Cobb angle measurements on spinal radiographs.

Our model deploys with one data labeling round (a rotating bounding box) and one training session. Then, the trained model accurately detects T1–L5 vertebral bodies on images and outputs the bounding box's four corner coordinates. In contrast, Sun et al.'s research requires two rounds of annotation to obtain the bounding box and its four corners, and two separate models (CenterNet, CenterNet2) must be trained [14]. Our model's processing speed far exceeds that of Sun's. While Sun's average processing time per image was 4.45 s, our model can perform vertebral body detection, Cobb angle calculation, visualization, and image saving in 2.2 s.

In automated Cobb angle detection, accurately locating the vertebrae and determining their upper and lower borders are crucial challenges. Traditional object detection algorithms identify horizontal bounding boxes that fail to reflect the inclination angle of the vertebrae [14, 17, 18]. To overcome this limitation, Sun's research proposed training a new model based on horizontal bounding boxes to obtain the vertebrae's four corner coordinates. Our model, however, considers object detection and relative angle as significant parameters. This method allowed our model to directly output the vertebrae's four corner coordinates, thus providing a more efficient solution to this problem.

Conclusion

In summary, we have devised an object detection-based deep learning algorithm that accurately measures the Cobb angle in pediatric patients with scoliosis. The algorithm exhibits remarkable performance and may potentially alleviate clinicians' workload in clinical settings. Nevertheless, our study had restrictions. Firstly, it involved a small imaging dataset. Secondly, the dataset originated from a single medical facility. Therefore, future research should focus on overcoming these limitations to enhance the precision and applicability of our deep learning model.

Supplementary Information The online version contains supplementary material available at https://doi.org/10.1007/s00586-023-08024-5.

Acknowledgements None.

Funding This work was supported by the National Research Foundation of Korea (NRF) grant funded by the Korean government (MSIT) (No. 00219725).

Declarations

Conflict of interest The authors have no financial or competing interests to disclose in relation to this work.

Ethical Approval The Institutional Review Board of Yeungnam University Hospital approved this study.

Informed Consent Informed consent was waived due to the retrospective nature of the study by the Institutional Review Board of Yeungnam University Hospital.

References

1. Lee GB, Priefer DT, Priefer R (2022) Scoliosis: causes and treatments. Adolescents 2:220–234
2. Malfair D, Flemming AK, Dvorak MF et al (2010) Radiographic evaluation of scoliosis: review. AJR Am J Roentgenol 194:S8-22
3. Choudhry MN, Ahmad Z, Verma R (2016) Adolescent idiopathic scoliosis. Open Orthop J 10:143–154
4. Donzelli S, Zaina F, Lusini M et al (2014) In favour of the definition "adolescents with idiopathic scoliosis": juvenile and adolescent idiopathic scoliosis braced after ten years of age, do not show different end results. SOSORT Award Winner 9:7
5. Wang J, Zhang J, Xu R et al (2018) Measurement of scoliosis Cobb angle by end vertebra tilt angle method. J Orthop Surg Res 13:223
6. Kinel E, Kotwicki T, Stryła W et al (2012) Corrective bracing for severe idiopathic scoliosis in adolescence: influence of brace on trunk morphology. Sci World J 2012:435158
7. Zhu Z, Xu L, Jiang L et al (2017) Is brace treatment appropriate for adolescent idiopathic scoliosis patients refusing surgery with cobb angle between 40 and 50 degrees. Clin Spine Surg 30:85–89
8. Kim JK, Choo YJ, Choi GS et al (2022) Deep learning analysis to automatically detect the presence of penetration or aspiration in videofluoroscopic swallowing study. J Korean Med Sci 37:e42
9. Kim JK, Wang MX, Chang MC (2022) Deep learning algorithm trained on lumbar magnetic resonance imaging to predict outcomes of transforaminal epidural steroid injection for chronic lumbosacral radicular pain. Pain Physician 25:587–592
10. Shin H, Choi GS, Shon OJ et al (2022) Development of convolutional neural network model for diagnosing meniscus tear using magnetic resonance image. BMC Musculoskelet Disord 23:510
11. Zhao ZQ, Zheng P, Xu ST et al (2019) Object detection with deep learning: A review. IEEE Trans Neural Netw Learn Syst 30:3212–3232
12. Bhandari A, Prasad PWC, Alsadoon A et al (2021) Object detection and recognition: using deep learning to assist the visually impaired. Disabil Rehabil Assist Technol 16:280–288
13. Yang R, Yu Y (2021) Artificial convolutional neural network in object detection and semantic segmentation for medical imaging analysis. Front Oncol 11:638182
14. Sun Y, Xing Y, Zhao Z et al (2022) Comparison of manual versus automated measurement of Cobb angle in idiopathic scoliosis based on a deep learning keypoint detection technology. Eur Spine J 31:1969–1978
15. Jin C, Wang S, Yang G et al (2022) A review of the methods on cobb angle measurements for spinal curvature. Sensors (Basel) 22:3258

16. Morrissy RT, Goldsmith GS, Hall EC et al (1990) Measurement of the Cobb angle on radiographs of patients who have scoliosis. evaluation of intrinsic error. J Bone Joint Surg Am 72:320–327
17. Pan Y, Chen Q, Chen T et al (2019) Evaluation of a computer-aided method for measuring the cobb angle on chest x-rays. Eur Spine J 28:3035–3043
18. Horng MH, Kuok CP, Fu MJ et al (2019) Cobb angle measurement of spine from X-ray images using convolutional neural network. Comput Math Methods Med 2019:6357171